UNIVERSITÀ DEGLI STUDI DI PADOVA

DIPARTIMENTO DI BIOLOGIA

Corso di Laurea in Biotecnologie

ELABORATO DI LAUREA

PENTOSE PHOSPHATE PATHWAY CONTROLS ENDOTELIAL-TO-MESENCHYMAL TRANSITION

Tutor: Prof. Massimo Santoro

Co-tutor: Cristina Arce Recatalá

Laureanda: Matilde Rizzi

ANNO ACCADEMICO 2022/2023

TABLE OF CONTENTS

FIGURE INDEX

TABLE INDEX

ABBREVIATION INDEX

6-AN	6-AMINONICOTINAMIDE
BBE	Bovine brain extract
BCA	Bicinchoninic acid assay
BSA	Bovine serum albumin
cm^2	Square centimetre
Ct	Threshold cycle
DNA	Deoxyribonucleic acid
dNTP	deoxyribonucleoside triphosphate
EC	Endothelial cell
ECL	Enhanced chemiluminescence
EndoMT	Endothelial-to-Mesenchymal transition
FAO	Fatty acid oxidation
FBS	Fetal bovine serum
G6P	Glucose-6-phosphate
G6PD	Glucose-6-phosphate dehydrogenase
$G6PD^{KD}$	Glucose-6-phosphate dehydrogenase knock-down
$G6PD^{OE}$	Glucose-6-phosphate dehydrogenase overexpression;
HRP	Horseradish peroxidase
HUVEC	Human Umbilical Vein Endothelial Cells
KD	Knock-down
mA	milliAmpere
mL	milliMetre
mM	milliMolar
NaClL	Sodium chloride
NADPH	Nicotinamide adenine dinucleotide phosphate
non-oxPPP	Non-oxidative phase of Pentose Phosphate Pathway
NP40 IGEPAL	Nonidet P-40 IGEPAL
OE	Overexpression
oxPPP	Oxidative phase of Pentose Phosphate Pathway
PBS	Phosphate-buffered saline
PGD	Phosphogluconate dehydrogenase
PGD^{KD}	Phosphogluconate dehydrogenase knock-down
PGD^{OE}	Phosphogluconate dehydrogenase overexpression
PPP	Pentose Phosphate Pathway
qPCR	Quantitative Real-Time polymerase chain reaction
RCF	Relative centrifugal force
RNA	Ribonucleic acid
ROS	Reactive oxygen species
RPM	Revolutions per minute
RT	Room temperature
SDS	Sodium dodecyl sulphate
SDS-PAGE	Sodium dodecyl sulphate-Polyacrylamide gel electrophoresis
shRNA	Short hairpin RNA
TBST	Tris buffered saline with Tween
TGF-β	Transforming growth factor β
Tris-HCl	TRIS Hydrochloride
V	Volt
ΔCt	Delta threshold cycle

1. ABSTRACT

Pentose phosphate pathway is a metabolic pathway parallel to glycolysis that has two main products: NADPH, which provides the reducing power for numerous anabolic reactions, and the ribose-5-phosphate, a precursor required for nucleotide synthesis. This metabolic pathway consists of an oxidative (oxPPP) and a nonoxidative phase (non-oxPPP). The oxidative phase involves a series of two irreversible reactions that are catalyzed by G6pd (Glucose-6-phosphate dehydrogenase) and Pgd (phosphogluconate dehydrogenase), respectively.

Endothelial-to-mesenchymal-transition (EndoMT) is a cellular process characterized by the loss of endothelial features and the acquisition of mesenchymal phenotype. EndoMT is a physiological condition required during cardiac development, but it can also be linked to a wide range of pathological conditions such as atherosclerosis, organ fibrosis and pulmonary hypertension. Recent studies showed a strong connection between EndoMT and endothelial metabolism, therefore we think that therapeutic manipulation of the endothelial metabolism could be a possible treatment for EndoMT-associated pathological.

Thanks to preliminary data from the laboratory, it has been shown that the blockade of the PPP pathway is linked to an increase of inflammation and EndoMT; hence, the thesis project is aimed to study the role of oxPPP pathway in controlling/modulating EndoMT.

To evaluate the contribution of oxPPP, we will characterize the EndoMT signature in cultured endothelial cells under oxPPP silencing using shRNA for *G6PD* and *PGD* or inhibiting PPP activity using 6-aminonicotinamide (6-AN). Furthermore, we will induce in cultured endothelial cells an overexpression of *G6PD* and *PGD* by viral infection. What we expect is to appreciate *in vitro* the transition from endothelial to mesenchymal features by western blot and qPCR supporting a novel function of this metabolic pathway in controlling EndoMT.

2. INTRODUCTION

2.1 PENTHOSE PHOSPHATE PATHWAY

The pentose phosphate pathway (PPP) is a metabolic pathway related to glycolysis that occurs in the cytoplasm of cells. It generates two main products: NADPH and ribose 5-phosphate. NADPH (nicotinamide adenine dinucleotide phosphate) is crucial for various cellular functions, including fatty acid synthesis and oxidative stress prevention, whereas ribose 5-phosphate is essential for nucleotide synthesis.

The PPP has two main phases: the oxidative branch (oxPPP) and the non-oxidative branch (non-oxPPP). The oxPPP phase consists of two irreversible oxidations that converts the glucose 6-phosphate (G6P, a product generated from the first reaction of glycolysis) into ribulose 5-phosphate. The key enzyme in this phase is glucose 6-phosphate dehydrogenase (G6pd), which allows the oxidation of G6P in 6-phosphogluconate and the releasing of NADPH, essential to maintain reduced glutathione involved in protecting against the reactive oxygen species (ROS). Another important enzyme is 6-phosphogluconate dehydrogenase (Pgd), which catalyzes the conversion of 6-phosphogluconate into ribulose-5-phosphate. The non-oxPPP branch involves a series of reversible reactions that interconvert various sugar phosphate molecules. The intermediates in this branch can be used for nucleotide synthesis or can be converted back into glycolytic intermediates to support energy production. One of the main products is ribose 5-phosphate.

The PPP pathway plays a crucial role in balancing the cell's need for NADPH and ribose 5-phosphate in EC metabolism. Such pathway can be activated in response to oxidative stress or during the oxidative burst to support massive NADPH requests in killing pathogens. Indeed, oxPPP-derived NADPH can be either antioxidant or pro-oxidant (TeSlaa et al., 2023). Its antioxidant function is the ROS removal which is an essential process to prevent many conditions such as cardiovascular diseases, cancer, inflammation but also aging. Its pro-oxidant role involves ROS production for cell signalling and antimicrobial killing during immune responses. Recently studies showed that the PPP pathway is also important in pathological conditions such as cardiovascular diseases, in which the oxidative stress plays an essential role, cancer and neurodegeneration diseases (Wood, 1985; Zimmer, 1992; Zimmer, 2001; Schaaff-Gerstenschlager & Zimmermann, 1993; Gupte, 2008; Mayr et al., 2008; Orešič et al., 2011; Vander Heiden et al., 2011; Riganti et al., 2012; Wallace, 2012).

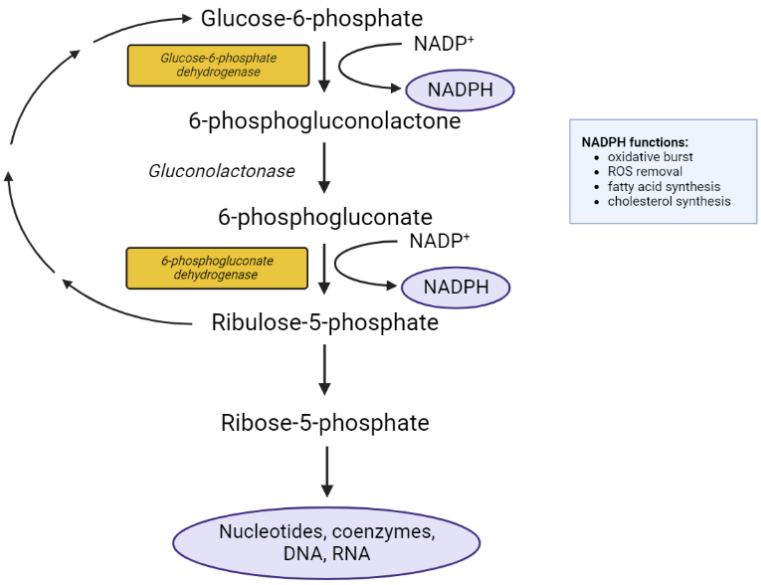

Figure 1: Summary scheme of the Pentose Phosphate Pathway

2.2 EndoMT

EndoMT is a biological process through which an EC undergoes a series of molecular events leading to significant phenotype changes: these include loss of EC rounded shape morphology, cell-to-cell contact, specific gene expression (e.g. *PECAM*, *vWF* and *CDH5*) and tissue barrier function. Such events occur while EC gains mesenchymal-like characteristics: spindle-shaped morphology, migratory behaviour, mesenchymal gene expression profile (e.g. *CNN1*, *FN1*, *FBLN5*, *VIM*, *MMP2*, *MMP10*, *COL4A1*, *PDGFRB*, *TAGLN* and *PLOD1*) and inflammatory properties.

EndoMT is mainly initiated by the endothelial transforming growth factor β (TGF-β) signalling. *TGF-β* signalling activates Smad2 through C-terminal serine phosphorylation (Schmiere and hill 2007; Derynck et al 2021). TGF-β /Smad2 activates mesenchymal genes (e.g *SNAIL*, *ZEB1* or *ZEB2*) and represses EC markers (e.g *PECAM*, *vWF* and *CDH5*). Although evidence has suggested that EndoMT is associated with diverse biological settings, including embryogenesis (Susienka and Medici, 2013) heart development (Welch-Reardon et al., 2015), also it is reported that whose continuous activation is required throughout the development and progression of various EndoMT-related vascular diseases. Some studies have shown the importance of EC metabolism in the regulation of EndoMT (Xiong et al., 2018). Indeed, recently studies showed the importance of FAO (fatty acid oxidation) in regulating EndoMT in EC (Lovisa and Kalluri, 2018), and eventually as a key driver of many different pathologies, such as atherosclerosis (C Souilhol, 2018), pulmonary hypertension (Suzuki et al., 2018), endocardial

fibroelastosis (Xu, Friehs, et al., 2015), and cardiac valvular disease (Kovacic MD, Dimmeler et al., 2019).

Nevertheless, EndoMT molecular mechanisms are not yet fully understood in physiological and pathological conditions. Moreover, no knowledge is available about the role of PPP in regulating EndoMT in EC. Research focused on this process may be fundamental to develop new targeted therapies for various diseases.

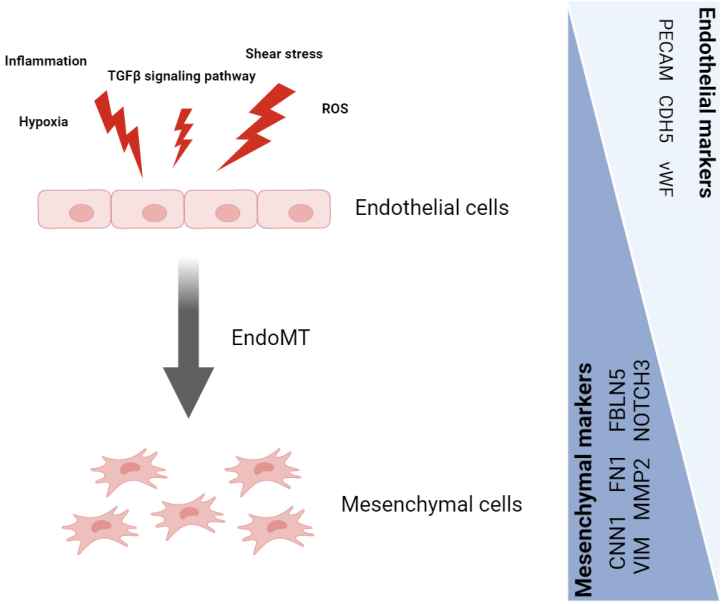

Figure 2: Schematic illustration of EndoMT process

3. AIM OF THE THESIS

The overall objective of the proposal is to study the role of endothelial oxPPP in controlling EndoMT. Our working hypothesis is that the oxPPP pathway have a protective role in EndoMT-associated diseases. By blocking oxPPP we will increase EndoMT and by overexpressing oxPPP we will decrease EndoMT marker, blocking or delaying the EndoMT-associated diseases.

To reach this overall objective, the project will focus at three specific AIMS:

(1) Characterization of EndoMT signature after blocking the *G6PD* activity in EC.
(2) Characterization of EndoMT signature after silencing *G6PD* and *PGD* in EC.
(3) To evaluate the protective role of oxPPP overexpression in EC.

4. MATERIALS AND METHODS

4.1 MATERIALS

4.1.1 HUVEC CELLS

Human Umbilical Vein Endothelial Cells (HUVEC) are primary EC obtained from Lonza (Cat. #00191027). The medium used for EC cultured was M199 complete. Its composition follows *(Table 1*). Once the medium complete was compound, it was filtered under the hood by a filter system with a membrane with 0,22µm pores.

HUVEC medium (complete)	Concentration	500mL	250mL
M199	80%	400mL	200mL
FBS	20%	100mL	50mL
BBE		1mL	0,5mL
Heparin 50mM		1mL	0,5mL
Penicillin-Streptomycin	1%	5mL	2,5mL

Table 1:HUVEC medium (complete)

4.2 METHODS

4.2.1 DEFROST HUVEC

It was removed the cryovial from the liquid nitrogen container and put it on dry ice. The vial was then immersed in a water bath (37°C) to thaw the cells and then add 10 mL of PBS 1X to clean the cells. The cells were centrifuged 4 minutes at 0.4 rfc at 21°C. Then, the supernatant was removed, and the pellet resuspended in 10mL medium for growth previously prepared. The HUVEC were cultured in 75 cm^2 cell culture flasks (15 ml medium pr. flask). The flasks were pre-coated with Gelatin 0.2% in PBS 1X. To prepare the gelatin, 1g of gelatin powder was dissolved in 500 mL of sterile PBS 1X. Once it is dissolved, 5mL of Penicillin-Streptomycin antibiotics 1X was added under the hood and eventually the gelatin was filtered. The HUVEC plating density is 5000-10000 cells per cm^2. The medium should be replaced every two days. At 80 -100% confluence, the cells were split at a 1:3 ratio. Then, the cells were seeded into 10 cm^2 plates (10 ml medium pr. dish) during experiments. Cells from passages 4-5 were used in all experiments. Note that cells from later passages may have changes in phenotype, and it is advised to discard cells beyond the 6th passage (Geraghty, Capes-Davis, 2014).

4.2.2 SUB-COLTURING HUVEC

When the 75 cm^2 cell culture flasks have reached 80%-100% confluency, they should be splitted into P100 (or 10 cm^2) petri dish to perform the experiments. Old medium was removed by aspiration, and the cells were washed with 10 mL PBS 1X two times. Trypsin-EDTA (5 mL) was added, and the 75 cm^2 cell culture flasks

were incubated at 37°C for 5 minutes. Cell detachment was checked under the microscope and the EC were visualized as round shaped cells. Complete medium (5 mL) containing 10 % FBS was added in order to inhibit further trypsin activity which may damage the cells. The cells were transferred to a Falcon tube of 15 mL and centrifuge 5 minutes at 4000 rcf at 21°C. The supernatant was discarded and resuspend the pellet in 10 mL of new medium previously prepared. Count the cells under a microscope with a hemocytometer or cell counter adding 10 µl of cells suspension and 10 µl Trypan blue in 1.5 mL Eppendorf. Fill the chamber with 10 µl of the 1:1 cell suspension, count the cell and calculate the number of cells and to seed according to the plating density. After the splitting, the plates have been checked every day to prevent contaminations. Every two days it was also necessary to replace the medium with new one.

4.2.3 6-AMINONICOTINAMIDE (6-AN) TREATMENT IN HUVEC

Preliminary data from the Laboratory showed a 50% blockade of the *G6PD* activity after 48h treatment with 6-AN and 75% of *G6PD* activity blockade after 72h treatment with 6-AN at different concentrations studied: 75µM, 150µM and 300µM (data not showed). For the present project we considered to proceed with 75µM during 72h.

For 6-AN (Sigma-Aldrich, Seoul, Korea) treatment, cells were seeded in P100 ($10cm^2$) and after 3h from the splitting the HUVEC were treated with 75µM of G6PD inhibitor 6-AN and incubated for 3 days. 72 hours after the treatment with the inhibitor, the cells were collected using the ice-cold RIPA lysis buffer.

4.2.4 HUVEC CELLS RECOVERING WITH RIPA LYSIS BUFFER

Per each plate, the medium was discarded, and the cells were washed three times by cold PBS 1X and scraped on ice in 80µL ice-cold RIPA buffer *(Table 2 and 3)*. Lysates cells were then collected in a 1,5 mL Eppendorf tubes and after pipetting up and down. Then, the lysates were centrifuged at 16000 rpm at 4°C for 10 minutes. The supernatant was therefore collected and put it at -80°C.

RIPA buffer 2X (50mL)	
20mM Tris-HCl pH 7.4	1mL of Tris-HCl pH7,4 1M
200mM NaCl	0,584g
2% SodiumDeoxycholate	1g in 50mL
0,2% SDS	0,5mL
2% NP40 IGEPAL	1mL in 50mL
Bring to 50mL with deionized H_2O	

Table 2: Ripa Buffer 2X (50mL) composition

RIPA MIX (100µL per P100)	
RIPA 2x	50µL
H_2O	36µL
Protease inhibitor 25x	10µL
Phosphatase inhibitor 10x	4µL

Table 3: RIPA mix composition per 10cm^2 petri dish (P100)

4.2.5 MEASUREMENT OF PROTEIN CONCENTRATION

The BCA Protein Assay kit (Pierce Biotechnology) was used to determine the protein concentration of the cell lysates.

Different concentrations of BSA (2 mg/mL stock solution) were used to prepare a standard curve (1mg/mL; 0.5 mg/mL; 0.25 mg/mL; 0.125 mg/mL 0.0626 mg/mL 0 mg/mL).
The samples were diluted 1:5 in RIPA buffer. Each sample was prepared in triplicates by adding 3 µL of the sample and 12 µL water MiliQ. Protein assay reagent A and protein assay reagent B were mixed 50:1 and 200 µl of the A + B solution was added to each 96-well plate. The 96-wells plate was incubated at 37ºC for 30 minutes before the absorbance was measured at 562 nm. The absorbance of the BSA standards (y-axis) was plotted against the known BSA concentrations (x-axis) and the protein concentration of the samples was determined.

4.2.6 SDS-PAGE (Sodium dodecyl sulphate-Polyacrylamide gel electrophoresis)

Polyacrylamide gel electrophoresis (PAGE) is the migration of proteins through pores in a polyacrylamide gel matrix in response to an electrical field.
The lysates were mixed with blue loading buffer Pack (3X) (Cell Signaling) and boiled for 5 minutes at 95°C. The ratio of lysates to loading buffer was 3:1.
Protein lysates were separated on 4–12% gradient SDS-PAGE (Thermo Fisher) gels at 110 V. The electrophoresis apparatus and pre-cast gel was assembled according to manufacturer's instructions (Bio-Rad). Running buffer *(Table 4)* was poured into the container, and equal amounts of protein were loaded into each well. Protein standards were loaded to marginal wells on both sides. The SDS-PAGE was run at 110 V until the bromphenol blue and protein standards reached the bottom of the gel.

MOPS 1X (Running Buffer)	
H_2O	950mL
MOPS 20X	50mL

Table 4: MOPS 1X (Running Buffer)

Proteins separated by SDS-PAGE must be transferred from the polyacrylamide gel to a nitrocellulose membrane by an electric current to make the proteins accessible for antibody detection. For each gel, one nitrocellulose membrane and four filter papers of the same size as the gel were cut. The nitrocellulose membrane was rinsed in transfer buffer (Table 5). The cassette was assembled in the following order: 2 filter papers, 1 sponge, nitrocellulose membrane gel, 2 filter papers, and 1 sponge. The red side of the cassette was inserted into the red anode of the blotting apparatus to allow the transfer of the negatively charged proteins in the gel to the membrane. A cooling block was placed into the container and the container was filled with cold transfer buffer. The transfer was conducted at 230 V and 300 mA for 120 minutes.

Transfer Buffer 1L	
Destilled water	600mL
Transfer Buffer 5X	200mL
Methanol (*)	200mL

Table 5: Transfer Buffer composition (1L)

(*) MeOH must be added under the chemical hood.

4.2.7 BLOCKING, ANTIBODY INCUBATION AND REVEAL

After the transfer, the membrane has been immersed in Ponceau red to stain for proteins to detect and record the pattern of protein bands. After capturing the images using ChemiDoc™ Imaging System (Bio-Rad), the membranes have been washed in TBST 1X 3 times for 5 minutes to remove the staining. Then, to avoid unspecific binding, the nitrocellulose membrane was blocked in 5% milk-TBST 1X for 60 minutes. After another 3X washing in TBST 1X for 5 minutes, the membranes were incubated with primary antibodies diluted in 3 % BSA-TBST at 4º Cover night on a shaker device. The next day, the membrane was washed 3 times for 5 minutes in TBST 1X to remove unbound antibody before the membrane was incubated with a HRP-conjugated secondary antibody diluted in 3% milk-TBST for 60 minutes on a shaker at room temperature. Next, the membranes were washed 3 times 5 minutes in 1X TBST and incubated with an ECL solution containing the substrates for HRP. The bands were visualized and acquired using ChemiDoc™ Imaging System (Bio-Rad). The band intensities of proteins were quantified using Image Lab software (Bio-Rad Laboratories). Following antibodies and dilutions were used for immunoblotting: β-actin (#691331, MP Biomedicals, 1:4000); pSMAD2 (#3101S, Cell Signaling, 1:1000); SMAD2t (#3103S, Cell Signaling, 1:1000); Calponin (#C6047, Sigma, 1:10000); VE-Cadherin (#AF1002, R&D, 1:1000); Fibronectin (#F3648, Sigma, 1:1000); SNAIL (#C15D3, Cell Signaling, 1:1000); ZEB1 (#NBP1-68930, Novus, 1:1000).

4.2.8 VIRUS TRANSDUCTION

The specific shRNAs for *G6PD* and *PGD* were obtained from Sigma-Aldrich (G6PD-targeting shRNA TRCN0000025817 and PGD-targeting shRNA TRCN0000028584). Recombinant lentiviruses carrying RNA for specific genes were produced by co-transfecting HEK293T cells with a mixture of plasmid DNA consisting of pMD2.G (Addgene, 12259), pMDLg/pRRE (Addgene, 12251) and pRSV-Rev (Addgene, 12253) using Lipofectamine 2000 Transfection Reagent according to the manufacturer's recommendations. In parallel, lentiviruses carrying the scramble RNA (Addgene, 17920) were produced. Supernatants containing virus were collected, passed through 0.45 μm filters and stored at −80 °C. Virus particles were quantified using Lenti-X p24 Rapid Titer kit (Takara, 632200). For in vitro modulation of oxPPP pathway, EC were infected with lentiviral vectors for 24 hours. Cells were collected 72 hours after the infection for biochemical analyses.

To induce the overexpression of *G6PD* and *PGD* on HUVEC, cells were plated in P100 (10 cm^2) petri dish and after three hours, the EC were infected with the lentiviruses. The following day, the medium was replaced. After 72 hours the cells were recovered in 1mL of TRIZOL®, according to manufacturer's instructions.

4.2.10 QUANTIFICATION OF GENE EXPRESSION

4.2.10-1 TOTAL RNA EXTRACTION

Total RNA from samples was isolated in appropriated RNAase free conditions to analyse gene expression of EndoMT and Endothelial markers and TGF-β signaling pathway. Per each 10 cm^2 culture plate, the medium was discarded, and the cells were washed three times by cold PBS 1X and scraped on ice in 1mL Trizol. Then, it was added 200 μL of Chloroform and mixed well by pipetting several times or by vortex, finally it was centrifuged 20 min at 12000 g at 4 °C.

Transfer the aqueous phase into a new 1.5 mL Eppendorf tube using a pipette and leaving behind some of the aqueous phase (about 1 mm above DNA layer to prevent DNA contamination). Then, add 500 μL of Isopropanol and mix the solution well. The solution containing the RNA was left at Room Temperature for 10 minutes, then centrifuged 10 minutes at 12000 g at 4°C. Discard the supernatant by inversion and resuspend the pellet in 75 % ethanol to wash the pellet and then, again centrifuged 5 minutes at 7500 g at 4°C. The ethanol was removed by inversion and the pellet was washed again with 75 % the ethanol. Discard the supernatant by inversion and air dry the pellet under the hood for 10 minutes. When it was dry, the pellet was resuspended in 20 μL.

The accuracy of gene expression is influenced by the quantity and quality of RNA. After RNA extraction, it was necessary determined the RNA concentration in each sample. RNA concentration and purity were determined spectrophotometrically using the NanoDrop 1000 and RNA integrity was assessed using a Bioanalyzer 2100.
The RNA thus obtained was then stored at -80 °C.

4.2.10-2 REVERSE TRANSCRIPTION

cDNA was synthesized by Real-Time Quantitative Reverse Transcription PCR (qRT-PCR). Following reagents were used to perform the Reverse Transcription: 10X RT Buffer 2 µL, 25X dNTP mix 0.8 µL, 10X RT Random primer 2 µL, Transcriptase 1 µL, RNAplus 0.1 µL and Nuclease-Free H_2O 4.1 µL. The reaction was carried out by the thermal cycler and settled as following: 10 min at 25 °C and 120 min at 37 °C. Then, the enzyme was inactivated 5 min at 85 °C. Synthetized cDNA was stored at -20 ºC or directly proceed to qPCR.

4.2.10-3 QUANTITATIVE REAL-TIME POLYMERASE CHAIN REACTION (qPCR)

Real-Time was then performed on CFX Real-Time PCR Detection System (Bio-Rad) preparing a Master mix of Hot fire EVA Green 2µL, Forward and Reverse primer 5 µM (2 µL), Nuclease-Free Water 5 µL and cDNA RT 1/10 (20ng/µL) 2 µL in a 384 multi-well plate. The cDNA was diluted 1/20 before adding to the PCR reaction. The cDNA was amplified following the manufacture's conditions: one initial Hold-step at 95 ºC for 10 min, a second step with 40 cycles including 15 seconds at 95 °C (denaturation) and 1 min at 60 °C (annealing/extension). The targets and reference (*ACTIN*) were amplified in parallel reactions.

Sequences for all primers were as follows:

GENE SYMBOL	**Gene name**	**FW**	**REV**
ACTIN	Actin	5'-CCA ACC GGG AGA AGA TGA-3'	5'-TCC ATC ACG ATG CCA GTG-3'
G6PD	Glucose-6-phosphate dehydrogenase	5'-GCA AAC AGA GTG AGC CCT TC-3'	5'-GAG TTG CGG GCA AAG AAG T-3'
PGD	Phosphogluconate dehydrogenase	5'-CGG ATC ATC CTC CTG GTG-3'	5'-ATG ATG TCA CCA GTA TCC AAC AA-3'
TGF-β1	Transforming growth factor-beta 1	5'-TTT TGA TGT CAC CGG AGT TG-3'	5-TGC AGT GTG TTA TCC CTG CT-3'
TGF-β2	Transforming growth factor-beta 2	5'-CCC TGC TGC ACT TTT GTA CC-3'	5'-CCA CTG GTA TAT GTG GAG GTG-3'

TGF-βR1	Transforming growth factor-beta receptor 1	5'-TGA TAT GAC AAC GTC AGG TTC TG-3'	5'-GAC CTT TGC CAA TGC TTT CT-3'
TGF-βR2	Transforming growth factor-beta receptor 2	5'-CAG CAT CAC CTC CAT CTG TG-3'	5'-GGG TCA TGG CAA ACT GTC TC-3'
CNN1	Calponin 1	5'-GAACATCGGCAACTTCATCAA GGC-3'	5'-GTACTTCACTCCCACGTTCACCTT-3'
FN1	Fibronectin 1	5'-CCATAAAGGGCAACCAAGAG-3'	5'-ACCTCGGTGTTGTAAGGTGG-3'
FBLN5	Fibulin 5	5'-CAGATTCCCACCAGTGCAAC-3'	5'-GGATCCAGGAACATTCGC-3'
PDGFRB	Platelet-derived growth factor receptor beta	5'-TGC AGA CAT CGA GTC CTC CAA C-3'	5'-GCT TAG CAC TGG AGA CTC GTT G-3'
TAGLN	Transgelin	5'-TCC AGG TCT GGC TGA AGA ATG G-3'	5-CTG CTC CAT CTG CTT GAA GAC C-3'
PLOD1	Procollagen-lysine-2-oxoglutarate 5-dioxygenase 1	5'-GCC GTT TGT GTC CCT GTT CTT C-3'	5'-ATG CTG TGC CAG GAA CTC TTC C-3'
COL4A1	Collagen type IV aplha 1	5'-CCTGGTCTTGAAAGGTGATAA G-3'	5'-CCCGCTATCCCTTGATCTC-3'
MMP2	Matrix metallopeptidase 2	5'-GGA ATG CCA TCC CCG ATA AC-3'	5'-CAG CCT AGC CAG CCA GTC GGA TTT-3'
MMP10	Matrix metallopeptidase 10	5'-CATTCCTTGTGCTGTTGTGTC-3'	5'-TGTCTAGCTTCCCTGTCACC-3'
CDH2	Cadherin 2	5'-ACCAGGTTTGGAATGGGACAG -3'	ATGTTGGGTGAAGGGGTGCTTG-3'
CDH5	Cadherin5	5'-GAA GCC TCT GAT TGG CAC AGT G-3'	5'-TTT TGT GAC TCG GAA GAA CTG GC-3'
PECAM	Platelet endothelial cell adhesion molecule	5'-AAG TGG AGT CCA GCC GCA TAT C-3'	5'-ATG GAG CAG GAC AGG TTC AGT C-3'
vWF	von Willebrand factor	5'-CCT TGA ATC CCA GTG ACC CTG A-3'	5'-GGT TCC GAG ATG TCC TCC ACA T-3'
SMAD2	Small mother against decapentaplegic	5'-GCCATCACCATCAAAACTGT-3'	5'-GCCTCTTGTATCCCACTGATCTA-3'
NOTCH3	Neurogenic locus notch homolog protein 3	5'-AGATTCTCATCCGAAACCGCT CTA-3'	5'-GGGGTCTCCTCCTTGCTATCCTG-3'
VIM	Vimentin	5'-AGG CAA AGC AGG AGT CCA CTG A-3'	5'-ATC TGG CGT TCC AGG GAC TCA T-3'
CXCL2	C-X-C Motif chemokine ligand 2	5'-CTGCTCCTGCTCCTGGTG-3'	5'-CTTAACCATGGGCGATGC-3'
IL6	Interleukin 6	5' – AAC CTG AAC CTT CCA AAG ATG G – 3'	5 – TCT GGC TTG TTC CTC ACT ACT – 3'
IL8	Interleukin 8	5' – TTG GCA GCC TTC CTG ATT – 3'	5' – AAC TTC TCC ACA ACC CTC TG – 3'
IL1β	Interleukin-1-beta	5'-CTG TCC TGC GTG TTG AAA GA-3'	5'-TTG GGT AAT TTT TGG GAT CTA-3'

ICAM	Intercellular adhesion molecule	5'-TCT GTG TCC CCC TCA AAA GTC-3'	5'-GGG GTC TCT ATG CCC AAC AA-3'
V-CAM	Vascular cell adhesion molecule	5'-GCT GCT CAG ATT GGA GAC TCA-3'	5-CGC TCA GAG GGC TGT CTA TC-3'
COL1A1	Gollagen type I alpha chain	5'-AAGAGGAAGGCCAAGTCGAG-3'	5'-CACACGTCTCGGTCATGGTA-3'

Table 6: Probes gene expression assay

4.2.10-4 ANALYSIS OF RESULTS

Threshold cycle (Ct) values were determined by QuantStudio Design & Analysis software. We normalized the gene expression with the levels of ACTIN mRNA; therefore, Ct values obtained from each gene were referenced to ACTIN and calculated ΔCt as the difference between gene of interest Ct value and the reference gene Ct value. ΔCt value was converted into the linear form using the term 2–ΔCt as a value directly proportional to the initial mRNA copy number (Livak & Schmittgen, 2001).

4.2.11 STATISTICAL ANALYSIS

The obtained results were analysed by GraphPad Prism 8 (GraphPad Software, Inc., San Diego, CA, USA). All results were expressed as mean ± Standard Error of Mean (SEM) for n determinations obtained from samples different.

For the analysis, one sample t and Wilcoxon test was applied. A p-value of less than 0.05 was considered significant. Statistical significance is reported as exact p-value.

5. RESULTS

5.1 INDUCTION OF ENDOMT SIGNATURE AFTER THE BLOCKING OF G6pd ACTIVITY IN HUVEC

To evaluate the role of oxPPP pathway in inducing EndoMT signature, HUVEC were treated with 6-aminonicotinamide (6-AN), a competitive inhibitor of *G6PD* activity, using 75 µM during 72 h.

The results showed that 6-AN-treated EC underwent a clear morphological transition adopting a more fibroblast or mesenchymal appearance. In the control images we can appreciate the physiological rounded shape of EC, whereas in the 6-AN-treated plate, the EC cells shape turns into a more elongated and fibroblast-like *(Figure 3A)*. Coincident with this morphological switch, 6-AN treatment of EC induced an increase in some mesenchymal markers such as calponin, however we did not show a significant change in fibronectin protein expression after 72h 6-AN treatment *(Figure 3B)*. Lastly, we investigated the endothelial marker Ve-Cadherin to confirm that EC after 6-AN treatment lost their EC distinguishing features. Strikingly, we did not find a decrease in Ve-Cadherin protein expression *(Figures 3C)*.

A

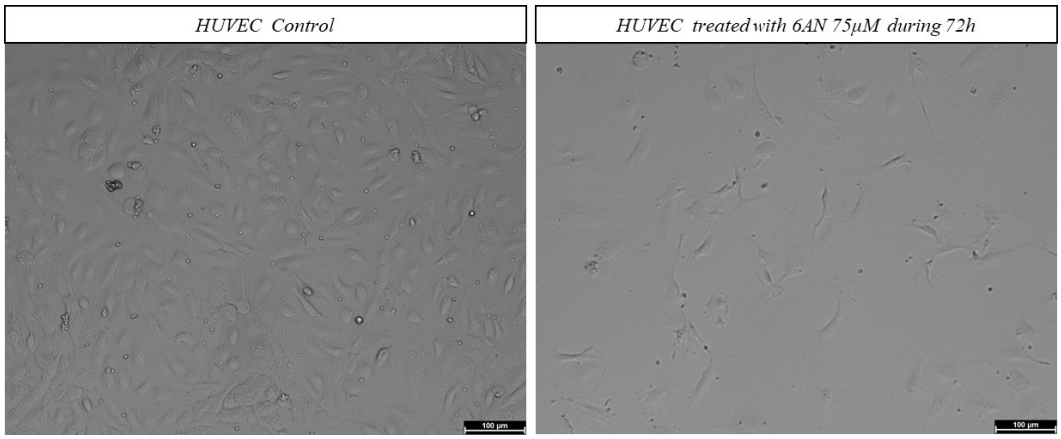

B

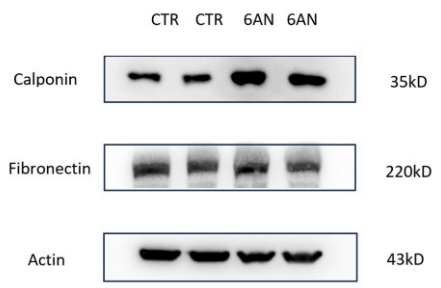

C

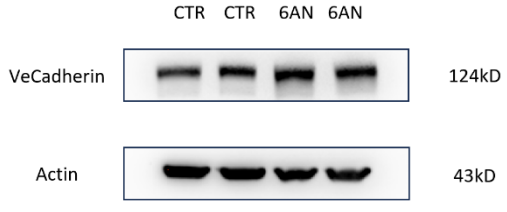

Figure 3: Induction of EndoMT after 6-AN 75 µM treatment during 72h
(A) 6-AN induce morphological changes consistent with EndoMT. (B) *G6PD* blocking activity inhibitor treatment induces the protein expression of EndoMT markers. (C) *G6PD* blocking activity inhibitor treatment do not change the protein expression of Ve-Cadherin EC markers.

Based on a previous strategy performed by Xiaolong Zhu (2023), we know that HUVEC could be stimulated to undergo EndoMT by treating these cells with TGF-β2 for 7 days. In fact, EndoMT is regulated by the TGF-β signaling pathway and Smad2 represents an important factor in this regulatory process, as its phosphorylation regulates EndoMT-related transcription factors to induce the EndoMT process. To investigate the role of oxPPP as potential novel mediator in the EndoMT process, we analyse if the G6pd blockade activity with 6-AN could modulate the downstream TGF-β signalling pathway and therefore modulate EndoMT process.

We found that after 6-AN treatment during 72 h there is an increased phosphorylation of the TGF-β downstream effector SMAD2, suggesting that inhibiting the *G6PD* activity acted to augment endogenous TGF-β signaling (Figure 4A). Moreover, the inhibition of *G6PD* activity increase the protein expression of the transcription factor Zeb1, but not Snail *(Figure 4B).*

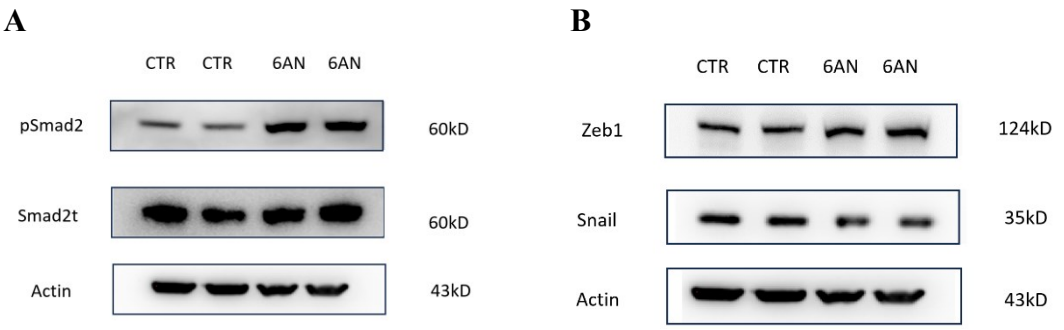

Figure 4: G6PD activity modulate in vitro TGF-β downstream Smad2 phosphorylation.
(A) Representative Western blot of phosphorylated Smad2 (pSmad2) in the presence or absence of 6-AN 75 µM for 3 days. (B) Representative Western blot of the transcription factors Zeb1 and Snail in the presence or absence of 6-AN 75 µM for 3 days.

5.2 *G6PD*^{KD} AND *PGD*^{KD} INDUCE EndoMT IN HUVECS

To evaluate the role of PPP in inducing EndoMT we knocked-down the expression of *G6PD* and *PGD* in EC. To do this, we infected HUVEC cells with a shRNA (short hairpin RNA) designed to stably knock down the expression of

G6PD or *PGD* (Moore, 2013). First, we validated the knock down of the two genes of interest, showing a significant reduction in the protein expression of *G6PD* and *PGD* compared to the scramble (SCR) or control (CTR) *(Figure 5A)*. Next, we analysed the EC with reduced PPP gene expression and the results exhibited a more fibroblast-like morphology in knocking down EC *(Figure 5B)* compared to SCR. Moreover, the results showed an activation of the EndoMT gene expression program after the knock-down of *G6PD* and *PGD (Figure 5C)* followed by a decrease in the endothelial phenotype markers only after G6PD^{KD}, but not after PDG^{KD} *(Figure 5D)*.

A

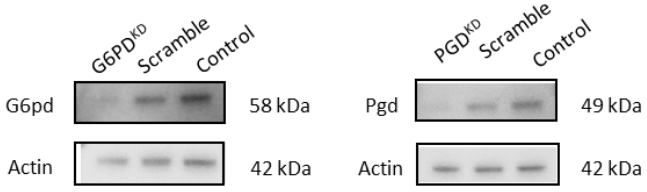

B

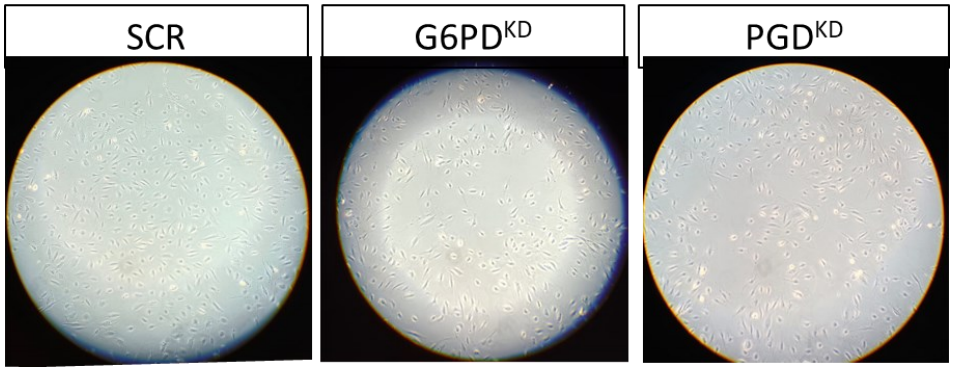

C

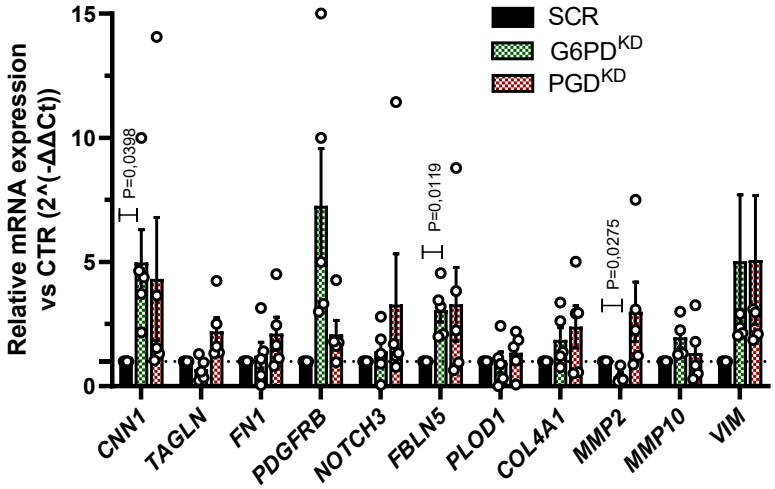

D

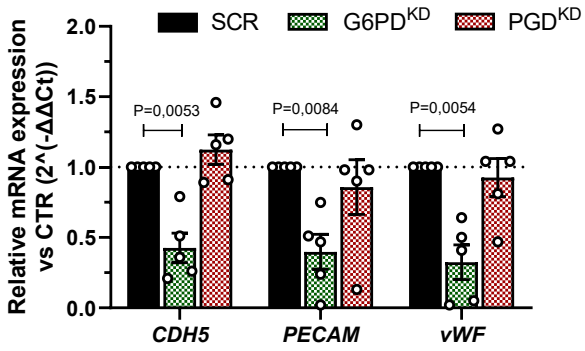

Figure 5: Induction of EndoMT after PPP knocking down.
(A) Representative Western blot of G6pd and Pgd protein expression after the PPP knocking down. (B) EC morphology following knockdown of *G6PD* and *PGD* (*G6PD*^{KD} and *PGD*^{KD}). (C) Knock-down of *G6PD* and *PGD* activates EndoMT program. (D) Knock-down of *G6PD* reduces EC markers, but not *PGD*. Data represents mean ± SEM with significance determined by one sample t and Wilcoxon test.

To better understand the mechanism of PPP^{KD}-induced EndoMT we analysed the gene expression of the TGF-β signalling pathway. Effectively, TGF-β family of ligands are important inducers of the transition from endothelial to mesenchymal-like cells. TGF-β markers can promote the downregulation of endothelial markers and consistent with that, the upregulation of mesenchymal markers in EC. Strikingly, *G6PD*^{KD} resulted in a reduction in TGF-β markers *(Figure 6A)*, whereas after the *PGD*^{KD} we observed an apparent increase in their mRNA levels, although not in a significant way *(Figure 6B)*.

A

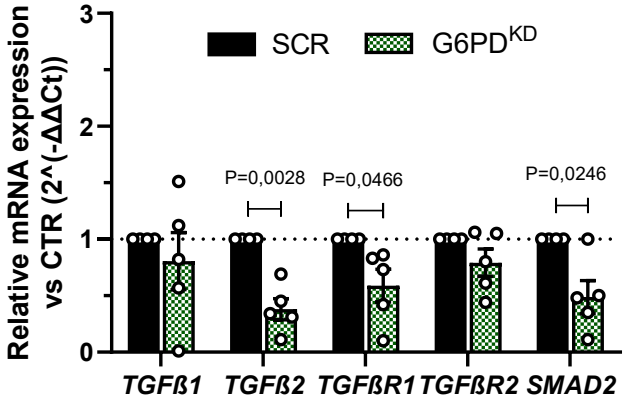

B

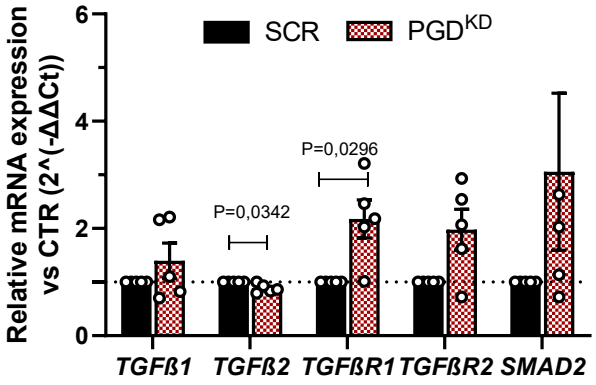

Figure 6: PPP modulate TGF-β markers.
(A) *G6PD*^{KD} decreases the gene expression of TGF-β signalling pathway. (B) whereas *PGD*^{KD} induce TGF-β signaling pathway. Data represents mean ± SEM with significance determined by one sample t and Wilcoxon test.

5.3 *G6PD*^{OE} AND *PGD*^{OE} RESCUE EndoMT IN HUVECS

To better understand the importance of PPP in the prevention of EndoMT program, we evaluated the maintenance of the endothelial phenotype thanks to the overexpression of the oxPPP. To perform this approach, we induced the overexpression of G6PD and PGD in EC infecting the HUVECs with a virus that included the specific overexpressed gene (*G6PD*^{OE} or *PGD*^{OE}). First, we verified that the overexpression worked by analysing G6pd and Pgd protein levels, the results showed an increase in the protein level of both the *G6PD*^{OE} and *PGD*^{OE} *(Figure 7A)*, as expected. Next, we examined the mRNA levels of the mesenchymal markers in *G6PD*^{OE} and *PGD*^{OE} to evaluate the protective role of oxPPP overexpressing in EC. The results showed that *G6PD*^{OE} and *PGD*^{OE} do not activate the EndoMT program *(Figure 7B)*. However, contrary to expectations, there is a decrease in endothelial markers after the overexpression of *G6PD* and *PGD (Figure 7C)*.

A

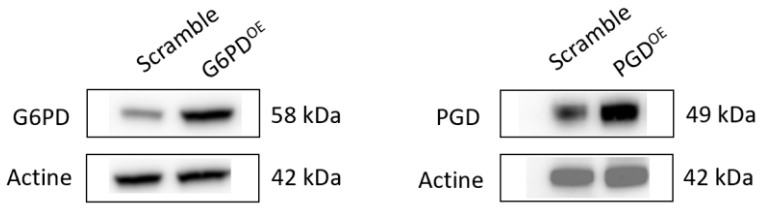

B

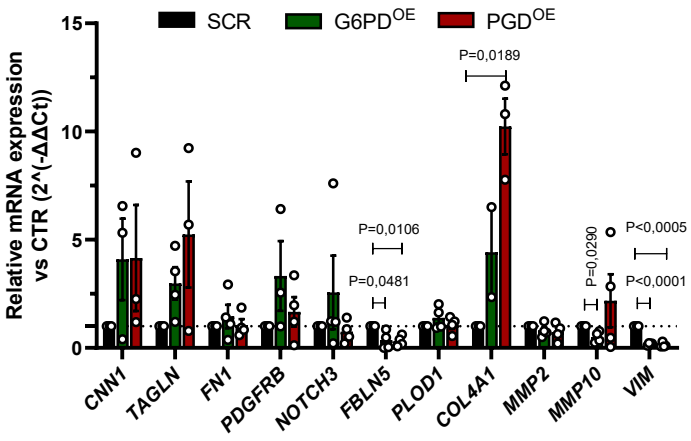

C

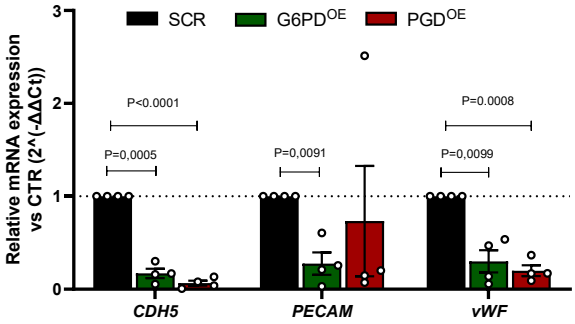

Figure 7: G6PDOE and PGDOE rescue EndoMT in HUVEC.
(A) Representative Western blot of G6pd and Pgd protein expression after the PPP overexpression. (B) *G6PD*^{OE} and *PGD*^{OE} do not activate EndoMT program in EC. (C) *G6PD* and *PGD* overexpression decrease EC markers. Data represents mean ± SEM, with significance determined by one sample t and Wilcoxon test.

To further understand the mechanism of the PPP overexpression in preventing EndoMT program we analysed the gene expression of the TGF-β signalling pathway. The oxPPP overexpression showed a decrease in the gene expression of TGF-β markers *(Figure 8A* and *Figure 8B)*, suggesting an important role of oxPPP overexpression in protecting from EndoMT.

A

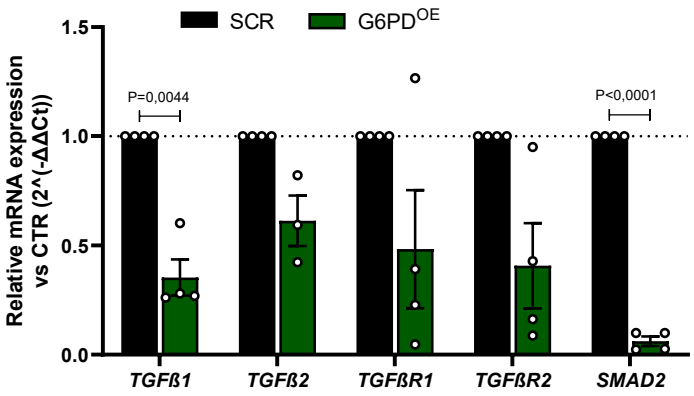

B

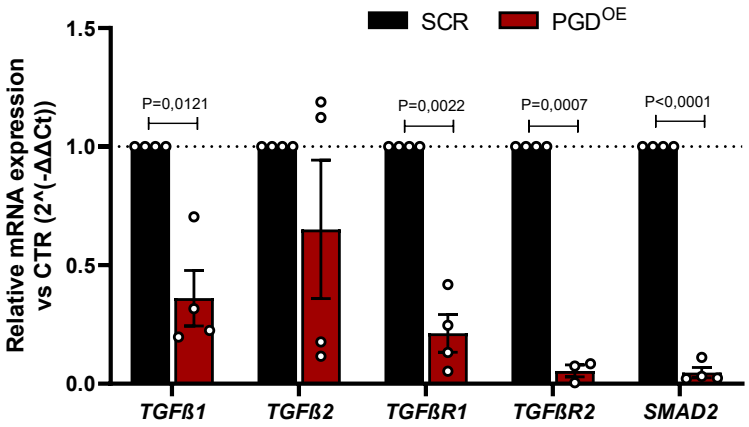

Figure 8: PPP modulate TGF-β signalling pathway.
(A) *G6PD^{OE}* decreases TGF-β markers, (B) and consistent with these results, also *PGD^{OE}* reduces TGF-β markers. Data represents mean ± SEM, with significance determined by one sample t and Wilcoxon test.

6. DISCUSSION

To date, cardiovascular diseases are becoming more and more frequent, and for this reason finding a solution is becoming a primary issue. Previous studies showed that EndoMT might contribute to several diseases including atherosclerosis, pulmonary hypertension, cardiac valve disease and organ fibrosis (Kovacic et al., 2012; Sanchez-Duffhues et al., 2016; Yang et al., 2017). Accordingly, to better understand the mechanism of the EndoMT process in both, physiological and pathological conditions, it is important to study the endothelial metabolism, which has been recently seen as a crucial modulator of EndoMT process (Zhu et al., 2023). In this regard, the results of our study showed for the first time that: (1) the oxPPP knock-down induces EndoMT program; (2) the suppression of G6PD activity also induces the expression of EndoMT markers; and (3) the up-regulation of the G6PD or PGD levels does not activate EndoMT program, indicating that G6PD or PGD might play an important role in preventing Endo-MT associated diseases.

EndoMT describes the process by which EC convert into mesenchymal cells in physiological and pathological conditions. Indeed, partial EndoMT it is reported in physiological and pathological conditions, such as cardiac fibrosis (Widyantoro et al., 2010), sprouting angiogenesis (Fang, Hultgren and Hughens, 2021) and many others, in which EC are not terminally differentiated into fibroblasts or mesenchymal cells, and both EC and mesenchymal markers can be transiently expressed by intermediate cells. Indeed, all the phenotypes in between the endothelial and the mesenchymal, are characterized by a different pattern of markers expression depending on the pathological conditions, the cell type and the duration of the treatment (Piera-Velazquez and Jimenez, 2019). It is therefore difficult to capture a complete EndoMT program in EC; the presence of cells that express different levels of both endothelial and mesenchymal markers is suggestive that EndoMT does occur. Our findings showed the induction of a partial EndoMT process after oxPPP blockade. Indeed, by knocking-down *PGD* or *G6PD* we observed an overall increase in EndoMT markers, although the only statistically significant ones were CNN1, FBLN5 and MMP2, revealing that the EndoMT was occurring. Moreover, G6PD silencing is accompanied by a decrease in endothelial markers such as PECAM, CDH5 and vWF, but not after PGD silencing, showing a major relevance of G6PD in the loss of the endothelial phenotype. Moreover, when we use 6-AN 75 μM for 3 days, an inhibitor of the PPP activity, we showed also a partial EndoMT signature, followed by an increase in Calponin protein expression, but not fibronectin. Moreover, regarding endothelial markers, we did not see a significant change in Ve-Cadherin expression, and this is most likely because the phenotype we obtained was an intermediate phenotype; to better validate the results, we should treat EC for a longer period to obtain a complete transformation from EC into mesenchymal cells. We think that it is important to highlight that

according to a recent study done by Daneshmandi et al., 2021, the pharmacological blockade of glucose 6-phosphate dehydrogenase (G6PD) using 6-AN at 10 μM for 3 days in Naïve $CD4^+$ T cells not only block G6pd activity also Pgd. This finding is highly relevant for our report, since the inhibition of both key enzymes allows oxPPP to be more consistently blocked. Hence, our next step it to check if the 6-AN treatment we performed at 75 μM for 3 days blocks both G6pd and Pgd also in EC.

Transforming growth factor β (TGF-β), is a multifunctional cytokine and one of the best studied EndoMT inducers. Indeed, increased TGF-β signalling has been suggested as a common underlying mechanism in almost every EndoMT-associated disorder (Ma et al., 2020). Therefore, blocking TGF-β signalling might be a promising therapy for EndoMT-related diseases. To better understand the mechanism of $oxPPP^{KD}$-induce EndoMT, and if the presence of oxPPP can prevent the EndoMT program by blocking TGF- β signalling pathway we analysed TGF-β markers mRNA levels. Oddly, we did not get the expected results: after G6PD silencing we can see a significant reduction of the TGF-β signalling, whereas after the PGD silencing showed no changes in TGF-β signalling, suggesting that $oxPPP^{KD}$-induced EndoMT could be independent of changes in the TGF-β signalling pathway gene expression. In contrast, after the suppression of the G6PD activity using the 6-AN, we showed an increase in the phosphorylation of the TGF-β downstream effector SMAD2 and Zeb1, suggesting that inhibiting the *G6PD* activity activate the downstream TGF-β signalling, without changes in the total RNA levels and therefore contributing to induce EndoMT program.

Since we demonstrated that PPP^{KD} plays a crucial role in inducing EndoMT, we further evaluated the possibility of preventing the EndoMT program after the overexpression of oxPPP. The results showed no changes in most of the mesenchymal markers compared to the control, suggesting that oxPPP do not activate EndoMT. However, we observe a significant reduction in the endothelial marker, suggesting that after the $oxPPP^{OE}$ the EC are undergoing some other changes and therefore more experiments should be performed to better understand this peculiar behaviour. Interestingly, the $oxPPP^{OE}$ can reduce the TGF-β signaling pathway, and therefore could prevent EndoMT program by reducing TGF- β levels.

PPP and glycolysis are two metabolic pathways tightly connected: in resting conditions, the glycolysis is predominant and only a small percentage of glucose ends up in the PPP, but in particular conditions such as oxidative stress, inflammation or other pathological conditions, the PPP has a greater impact than glycolysis and this is why previous reports showed that by blocking PPP, we induce glycolysis (TeSlaa et al., 2023). A recent study performed by Zhu et al. discovers some peculiar metabolic rewiring of EC while they undergo TGFβ-induced EndoMT. The study points out that chronic TGF-β stimulation of human EC leads

to an increase in glucose uptake via GLUT1 expression and augmented pyruvate production. TGF-β signaling acts by repressing the expression of PDK4, a key inhibitor of PDH-dependent Acetyl-CoA (Ac-CoA) biosynthesis. Indeed, the authors found that TGF-β-mediated inhibition of the PDK4 enzyme leads to an increase in Ac-CoA synthesis. The authors describe a novel role for acetate and ACC2 in regulating EndoMT and atherosclerosis via modulation of the TGF-β signaling. For these reasons, our next step is evaluate the acetyl-CoA levels after oxPPP knock-down or suppressing the oxPPP activity. Moreover, we would like to evaluate if Acetate can rescue $oxPPP^{KD}$-induced EndoMT (Simons et al., 2023; Recatalá and Santoro, 2023)

In summary, our work reveals a novel role of endothelial metabolism in controlling EndoMT; which suggests new potential targets for therapeutic approaches for various human disorders mediated by EndoMT, such as pulmonary hypertension, metastatic spread of tumors, atherosclerosis, organ fibrosis and other pathological conditions.

7. CONCLUSION

In this study we investigated the role of oxPPP in modulating EndoMT and we achieved the following conclusions:

(1) We showed a partial EndoMT signature after the blockade of *G6PD* activity in EC firstly by observing a clear morphological change. Next, we also found an increase in mesenchymal markers, confirming our hypothesis.

(2) Moreover, we characterized the induction of EndoMT after G6PD and PGD knock-down, showing the crucial role of oxPPP in inducing EndoMT.

(3) We revealed the protective role of oxPPP overexpression in EC, preventing the EndoMT. We envision oxPPP overexpression as a novel therapeutic strategy in numerous EndoMT-related diseases.

7. BIBLIOGRAPHY

1. Li X, Sun X, Carmeliet P. Hallmarks of Endothelial Cell Metabolism in Health and Disease. Cell Metab. 2019 Sep 3;30(3):414-433. doi: 10.1016/j.cmet.2019.08.011. PMID: 31484054.
2. Ma J, Sanchez-Duffhues G, Goumans MJ, Ten Dijke P. TGF-β-Induced Endothelial to Mesenchymal Transition in Disease and Tissue Engineering. Front Cell Dev Biol. 2020 Apr 21;8:260. doi: 10.3389/fcell.2020.00260. PMID: 32373613; PMCID: PMC7187792.
3. Piera-Velazquez S, Jimenez SA. Endothelial to Mesenchymal Transition: Role in Physiology and in the Pathogenesis of Human Diseases. Physiol Rev. 2019 Apr 1;99(2):1281-1324. doi: 10.1152/physrev.00021.2018. PMID: 30864875; PMCID: PMC6734087.
4. Pinto MT, Ferreira Melo FU, Malta TM, Rodrigues ES, Plaça JR, Silva WA Jr, Panepucci RA, Covas DT, de Oliveira Rodrigues C, Kashima S. Endothelial cells from different anatomical origin have distinct responses during SNAIL/TGF-β2-mediated endothelial-mesenchymal transition. Am J Transl Res. 2018 Dec 15;10(12):4065-4081. PMID: 30662651; PMCID: PMC6325528.
5. Stincone A, Prigione A, Cramer T, Wamelink MM, Campbell K, Cheung E, Olin-Sandoval V, Grüning NM, Krüger A, Tauqeer Alam M, Keller MA, Breitenbach M, Brindle KM, Rabinowitz JD, Ralser M. The return of metabolism: biochemistry and physiology of the pentose phosphate pathway. Biol Rev Camb Philos Soc. 2015 Aug;90(3):927-63. doi: 10.1111/brv.12140. Epub 2014 Sep 22. PMID: 25243985; PMCID: PMC4470864.
6. TeSlaa, T., Ralser, M., Fan, J. *et al.* The pentose phosphate pathway in health and disease. *Nat Metab* 5, 1275–1289 (2023)
7. Theodorou K, Boon RA. Endothelial Cell Metabolism in Atherosclerosis. Front Cell Dev Biol. 2018 Aug 7;6:82. doi: 10.3389/fcell.2018.00082. PMID: 30131957; PMCID: PMC6090045.
8. Xian S, Chen A, Wu X, Lu C, Wu Y, Huang F, Zeng Z. Activation of activin/Smad2 and 3 signaling pathway and the potential involvement of endothelial-mesenchymal transition in the valvular damage due to rheumatic heart disease. Mol Med Rep. 2021 Jan;23(1):10. doi: 10.3892/mmr.2020.11648. Epub 2020 Nov 12. PMID: 33179113; PMCID: PMC7673319.
9. Xiong J, Kawagishi H, Yan Y, Liu J, Wells QS, Edmunds LR, Fergusson MM, Yu ZX, Rovira II, Brittain EL, Wolfgang MJ, Jurczak MJ, Fessel JP, Finkel T. A Metabolic Basis for Endothelial-to-Mesenchymal Transition. Mol Cell. 2018 Feb 15;69(4):689-698.e7. doi: 10.1016/j.molcel.2018.01.010. Epub 2018 Feb 8. PMID: 29429925; PMCID: PMC5816688.
10. Yoshimatsu, Y., Watabe, T. Emerging roles of inflammation-mediated endothelial–mesenchymal transition in health and disease. *Inflamm Regener* 42, 9 (2022). https://doi.org/10.1186/s41232-021-00186-3